Real time mapping of corrosion activity under coatings

M. Khobaib*,[1], A. Rensi[2], T. Matikas, M.S. Donley

*Air Force Research Laboratories, Materials and Manufacturing Directorate, Nonmetallic Materials Division,
Coatings Research Group, Wright–Patterson AFB, OH 45433-7750, USA*

Abstract

Current accelerated testing of aircraft coating systems for corrosion protection relies heavily on salt spray methods. Electrochemical techniques such as electrochemical impedance spectroscopy (EIS) and electrochemical noise methods (ENM) provide insight into the global properties of a coating system, and both techniques are being used on a limited basis. However, there is a need to investigate corrosion events with greater spatial resolution under coatings at the metal/coating interface. Such corrosion activity may be related to coating defects and variations in the surface chemistry of the underlying metal.

The scanning vibrating electrode technique (SVET) has been developed to allow high spatial resolution investigation of localized corrosion activity that may be associated with coating defects or galvanic coupled regions of the metal surface. The SVET offers high resolution in current measurements of the order of 0.5 $\mu A/cm^2$ and is able to detect in-situ initiation and progress of corrosion activity under a protective coating. Using the SVET, minute variations in d.c. current associated with localized corrosion activity are detected and used to map both anodic and cathodic corrosion activities in a localized area. The difference in initial corrosion activity under various coatings can be correlated to the performance life of the coatings. The application of SVET to aircraft coatings and corrosion is reported to demonstrate the utility of this important new electrochemical tool.

In the current study, the SVET was used to discriminate the corrosion protection performance of selected sol–gel based coating systems. Sol–gel based surface treatments are being developed as part of an environmentally compliant coating system alternative to the currently used chromate-based systems. The SVET results are compared with data obtained from chromium inhibition coating systems. The SVET analyses are compared with electrochemical impedance measurements. The comparison of such data will provide the basis to adopt SVET measurements as an early performance discriminator for newly developed coating systems. © 2001 Elsevier Science B.V. All rights reserved.

Keywords: Corrosion activity; Real time mapping; Electrochemical impedance spectroscopy; Electrochemical noise methods; Scanning vibrating electrode technique; Sol–gel based coating systems

1. Introduction

One of the main requirements of aircraft coatings is to provide corrosion protection to aluminum-skinned aircraft structures. Aircraft coatings provide such protection through a complex mechanism of inhibition and barrier functionality. In this scheme of corrosion prevention, the surface pretreatment provides passivation of the metal surface, incorporates corrosion inhibitors, and creates a surface topography for maximum primer coating adhesion. The organic primer coating also incorporates corrosion inhibitors and serves as an adhesive layer between the metal substrate and the top coat layers. At mechanically stressed or damaged areas such as fasteners, rivets, expansion joints and scratches, the surface pretreatment/primer system provides active corrosion protection from exposure to environmental factors (e.g., water, acid, and solvent). The surface treatment/primer coatings are intended to remain intact throughout the entire programmed depot maintenance cycle. The loss of coating integrity, mainly due to loss of adhesion, results in corrosion initiation. Other factors contributing to corrosion initiation include defects, pores in the primer coating, polymer degradation and resulting changes in transport properties of primer coatings that allow the ingress of environment to the substrate. Lastly, a corrosion prone multi-component metallic surface in case of Al 2024-T3 also contributes to corrosion initiation. All these factors can be, in a broader sense, classified as loss of adhesion at the primer/surface pretreatment interface. Such loss of adhesion to the substrate is a key element in the corrosion initiation process.

Several conventional ex-situ techniques have been used to study the corrosion process occurring under the coating,

---

* Corresponding author. Tel.: +1-937-255-9050; fax: +1-937-258-8075.
E-mail address: mohammad.khobaib@afrl.af.mil (M. Khobaib).
[1] Address: University of Dayton Research Institute, 300 College Park, Dayton, OH 45469-0168, USA.
[2] Address: University of Dayton Research Institute, 300 College Park, Dayton, OH 45469-0168, USA.

but these methods have their own inherent problems [1]. Polarization is destructive to the sample, electrochemical impedance spectroscopy (EIS) imposes an external voltage and electrochemical noise method (ENM) cannot identify the corrosion site, as is also the case with the other techniques. Furthermore, because each sample has its own unique characteristics, ex-situ techniques require several samples to be exposed for various lengths of time. Many measurements must be repeated to accumulate statistical data to account for the random nature of the coating defects and corrosion processes. Also, because initiation times are often uncertain, growth rates of localized corrosion are particularly difficult to determine. These limitations, coupled with uncertainties in defects due to processing, make comparison of various types of coatings difficult [1–3].

The SVET has been developed to allow in-situ examination of localized corrosion activity through the detection of minute d.c. current variations associated with corrosion. The technique offers high resolution in current measurements of the order of $0.5\,\mu A/cm^2$ and is able to detect the initiation and progression of corrosion activity under a protective coating. A video image of the sample, captured after each scan, pinpoints the site of corrosion initiation, and calculated current density vectors can be superimposed on the video image to determine the precise location of a corrosion current source. A repeat scan function quantifies corrosion progression with time by allowing the user to choose multiple consecutive scans and observe the growth or repassivation of corrosion sites. The difference in initial corrosion activity under various coatings is expected to influence the failure life of the coatings. In the current study, this technique was used to discriminate the corrosion resistance performance of selected sol–gel based coatings. The sol–gel based system is being developed as an environmentally compliant alternative to the currently used chromate based coating systems. The results are compared with data obtained from chromium inhibition coating systems. The SVET analyses are compared with electrochemical impedance measurements. The comparison of such data will provide the basis to adopt scanning vibrating probe measurements as an early discriminator of newly developed coating systems.

2. Experimental details

The SVET tests were conducted using Applicable Electronics Model 1200. High strength Al 2024-T3 was selected as the substrate for all the test panels. Initially a water based epoxy cross-linked with a polyamine curing agent coated panel was scribed and exposed to Prohesion chamber to create visible corrosion damage. The other four systems consisted of another proprietary water based polyamine cross-linked coating, a commercial proprietary E-coat, a Lord Aeroglaze sol–gel and a 40% epoxide sol–gel coating over a chromate conversion treated substrate. The E-coat and Lord Aeroglaze sol–gel primed surface were treated with a polyurethane top coat. In all cases, the coating film thickness was around $40\,\mu m$. These coatings were exposed to Harrison's solution $-3.5\,wt.\%$ $(NH_4)SO_2 + 0.5\,wt.\%$ NaCl and the local current density maps were generated over different periods of exposure. A $5 \times 5\,mm^2$ area was selected for SVET scans. The probe height was maintained at approximately $75\,\mu m$ in all the experiments.

Initially the results were obtained on a scribed coated panel which had gone through a 2000 h Prohesion cycle. The area selected for the SVET scan on the coated panel was at a distance from the scribe but included a small section of known delaminated area. The probe was positioned in such a way that approximately half of the scanned region contained delaminated coating and the remaining half contained intact coating. The other specimens studied were intact (with no artificial damage) and the progress of corrosion activity was recorded by scanning number of small areas of each coated sample. The cell was formed by gluing a 1/8″ high 3/4″ diameter circular plastic tube on top of the coated sample. The electrolyte used was regular Harison's solution. All the measurements were made at open circuit potential. The first scan was taken after 1 h of exposure, followed by 5, 48, 288, 1056 and longer hours.

3. Results and discussions

Fig. 1 shows an optical photograph of a proprietary water based epoxy coating which was scribed to create damage

Fig. 1. Optical photograph of a cracked coating.
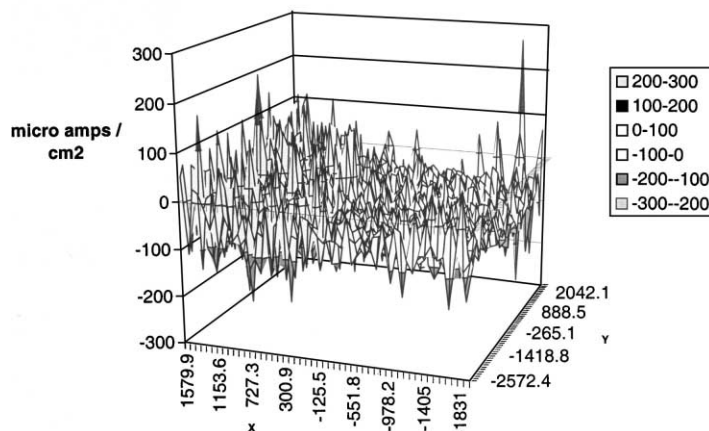
SVP Mapping of Coating: 3-D Plot

Fig. 2. 3-D current density map of the delaminated area (the units of *X* and *Y* axes are in micrometers).

in the coating and then exposed to the Prohesion chamber for 2000 h to produce corrosion damage and coating degradation. As a result, extensive corrosion and coating damage was present in the vicinity of scribe. However, it also provided a large area of undamaged coating as can be seen in Fig. 1. Much of the delamination of the coating occurred in and around the area of the scribe. An area adjacent to the scribe, such that half of the scanned area contained delaminated coating and the remaining half contained only intact coating, was selected for SVET and EIS study. Fig. 2 shows the current density map of the sample surface. The *X* and *Y* axes

represent locations of the surface area scanned in microns, while the *Z*-axis represents current density ($\mu A/cm^2$). Here, the convention of anodic current density showing positive current density is chosen, which is indicative of corrosion active site. From the 3-D map, anodic current density was observed to occur over approximately half of the sample.

In order to establish a one-to-one correspondence with the corrosion current measurement and the active sites in the coating, the 3-D surface plot was transformed into a 2-D plot and placed in 1:1 correspondence next to the video image of the sample captured immediately following the scan. Fig. 3a
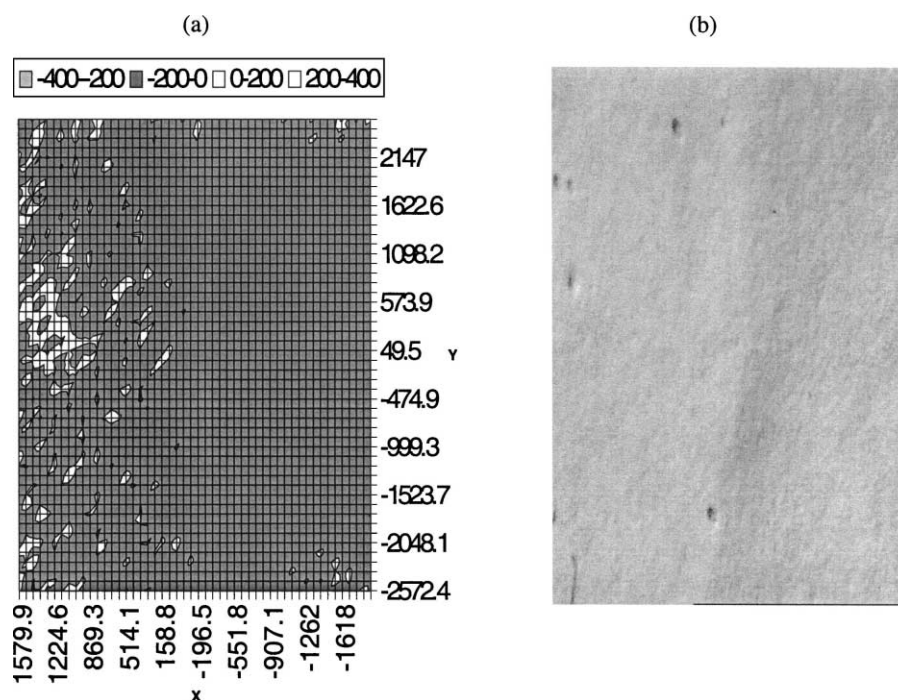

Fig. 3. (a) 2-D current density map, units of *X* and *Y* axes are in micrometers; (b) video image of the scanned surface.
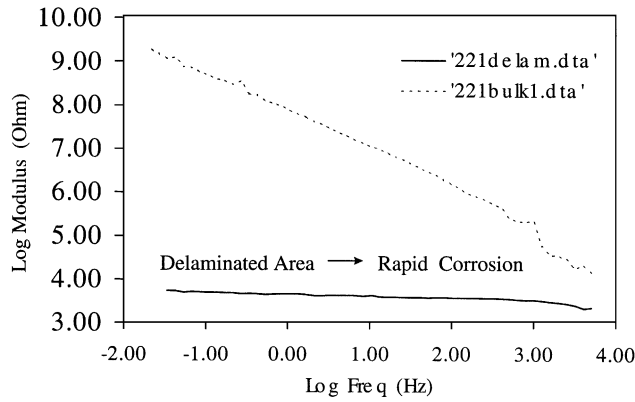
Fig. 4. Bode plots from intact and delaminated area of the coating.

and b compares the 2-D current density map with the video image of the area scanned, as indicated. As shown in Fig. 3b, a ridge is apparent in the center of the in-situ video image. The delaminated portion is located to the left of the ridge, while the intact coating is located to the right of the ridge. When compared with the 2-D plot shown in Fig. 3a, anodic current shows up in the delaminated region only. These data suggest that conductive pathways were present only in the delaminated region. This coating system appears to provide an effective barrier to corrosion attack only in the absence of scratches or substantial defects.

Bode plots obtained from these two different locations (intact and delaminated) are presented in Fig. 4. The dashed line, denoted as 221*bulk*1.*dta*, represents the intact portion of the coating while the solid line, 221*delam.dta*, represents the delaminated area in the coating. The difference in the barrier resistance extrapolated from the low frequency value clearly shows 4–5 orders of magnitude difference in impedance values. These data also confirm the difference in corrosion activities between intact and delaminated areas.

Fig. 5a and b shows the progress of corrosion with exposure time for a water based epoxy coated panel. The current activity is similar, but the level of the current density at the most active site is over $700 \mu A/cm^2$ as shown in Fig. 5a, which increased to nearly $1250 \mu A/cm^2$ after 18 h of exposure, as shown in Fig. 5b. These data suggest an increase in current activity with extended exposure to Harrison's solution. The corrosion current continued to increase with longer exposure time, indicating the presence of conductive pathways in the coating. Although the results are obtained from a small $5 \times 5 mm^2$ area, these data are typical of many scans obtained over different portions of the same panel.

The situation is quite different as shown in Figs. 6 and 7 for an E-coat chromate conversion coated and a sol–gel based coating system. The current density map of an E-coat chromate conversion coated sample on Al 2024-T3 is shown in Fig. 6. The anodic current activity after initial exposure of 1 h is quite high, of the order of $1500 \mu A/cm^2$ as shown in Fig. 6a, with a lot of cathodic activity. The value of anodic current density drastically falls to just over $200 \mu A/cm^2$ after an extended exposure of 48 h. The cathodic activity appears
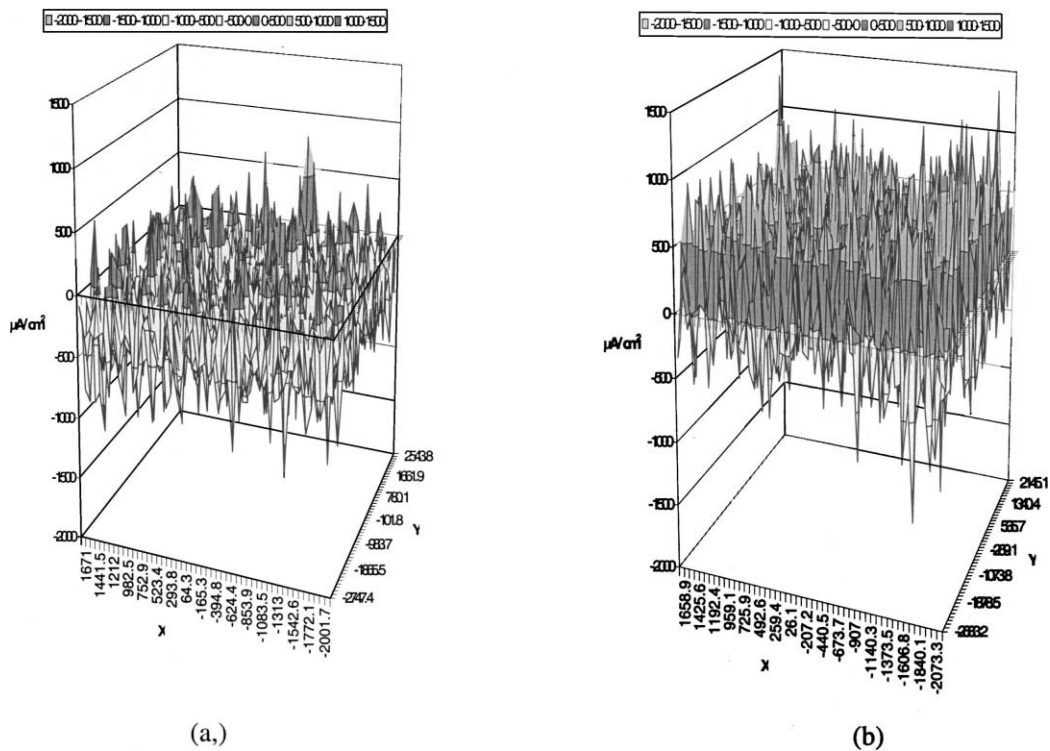

(a,)

(b)

Fig. 5. 3-D current density maps showing progress of corrosion activity with exposure — units of X and Y axes are in micrometers: (a) 5 h exposure; (b) 18 h exposure.
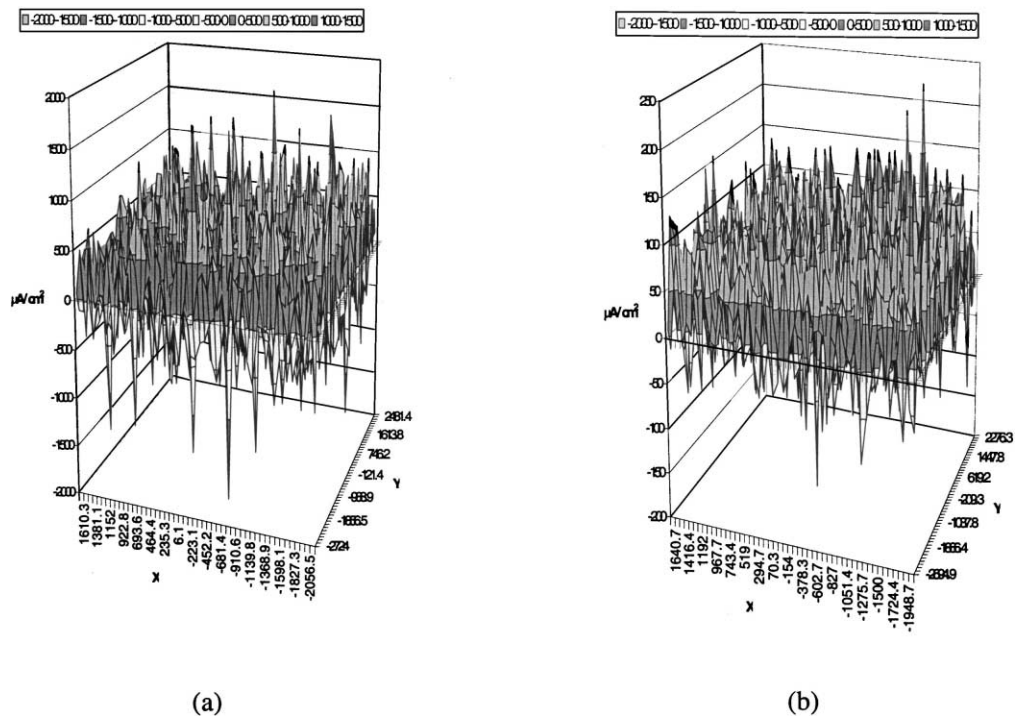
Fig. 6. 3-D current density maps of an E-coat chromate conversion coated coatings exposed to Harrison's solution — units of *X* and *Y* axes are in micrometers: (a) 5 h; (b) 18 h.
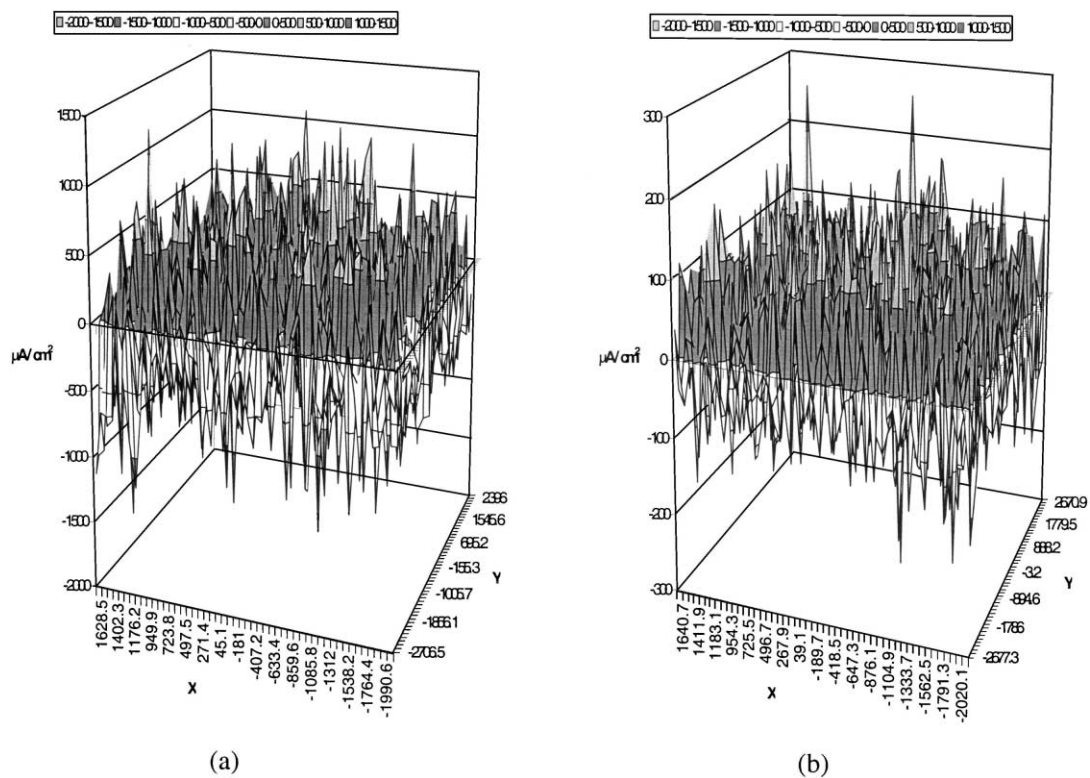

Fig. 7. 3-D current density maps of a sol–gel based coating showing a decrease in current density with exposure time — units of *X* and *Y* axes are in micrometers: (a) 1 h; (b) 48 h.
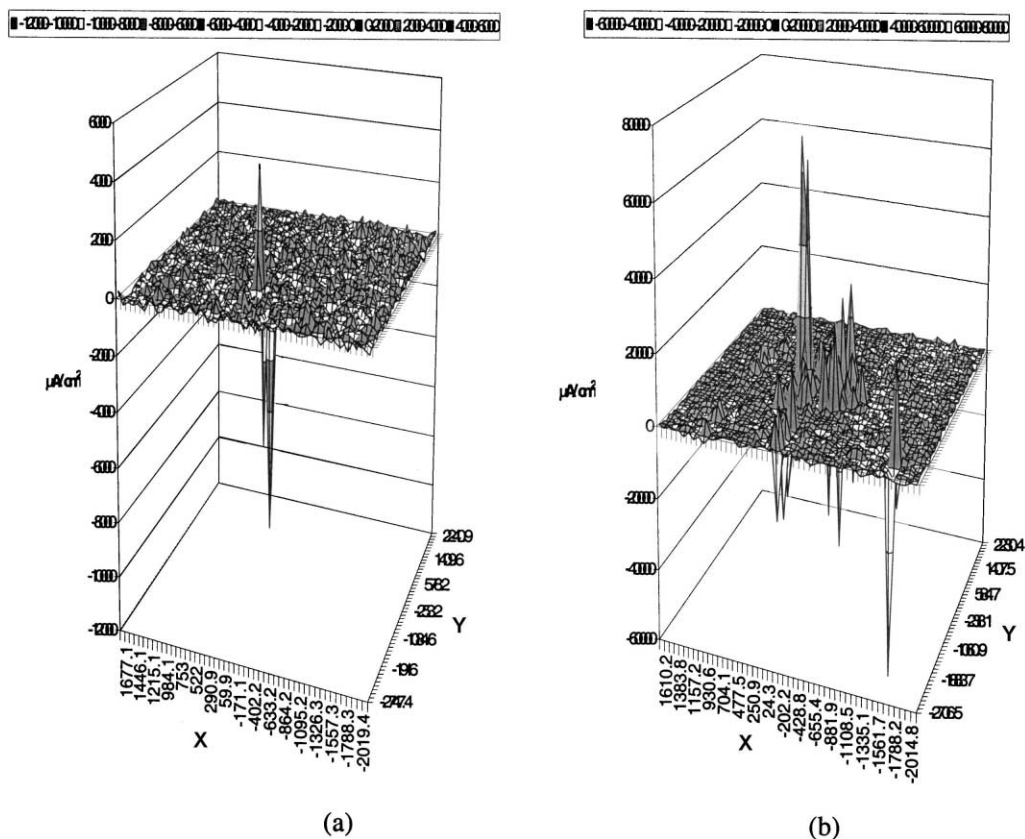
Fig. 8. 3-D current density maps of a 40% epoxide sol–gel coating showing increase in current activity with increasing exposure — units of *X* and *Y* axes are in micrometers: (a) 288 h; (b) 1056 h.

to decrease as well. A similar situation was observed with a sol–gel coated panel, as shown in Fig. 7. The anodic current density at the most active site is over $1000\,\mu A/cm^2$ as shown in Fig. 7a, after an initial exposure of 1 h in Harrison's solution. The value of this current density decreased to around $220\,\mu A/cm^2$ as shown in Fig. 7b after an extended exposure of 48 h. Both these data suggest a decrease in current activity as well as conductive pathways after extended exposure. It is postulated that such a decrease in corrosion current with exposure time is the result of filling the pores in the coating as well as passivation of the active corrosion sites.

A decrease in barrier resistance with extended exposure time was reported for conventional and experimental high performance Air Force aircraft coatings [4,5]. Similar explanations based on active site passivation and pore filling were put forward for those observations. Again, it should be noted that the first few days of exposure does not necessarily provide a guide for the life prediction of a coating [5]. Although both of these coatings, as shown in Figs. 6 and 7, exhibited very similar corrosion behavior to SVET results obtained from an initial exposure of a few days, the corrosion behavior was found to be drastically different over an extended exposure [6]. The sol–gel coating system showed visible signs of degradation after 3 months exposure to alternate immersion in regular Harrison's solution combined with cyclic ultra

violet chamber and Prohesion exposure. At this time, we are not able to correlate these data to any life cycle performance.

After the observations cited above, panels were prepared in our laboratory with a 40% epoxide sol–gel coating. Such a coating is very tenacious but has a high degree of cracking propensity under exposure to corroding environments such as water and saline solution. Fig. 8a and b show the 3-D current density maps obtained from these coatings after exposure to Harrison's solution. Initially, the current activity was very small and even after 288 h of exposure, a current density of under $2000\,\mu A/cm^2$ was observed as shown in Fig. 8a. At the same time, the corrosion was very localized. However, over an extended exposure of 1056 h the corrosion activity increased and the same previous active site produced a current density of over $5000\,\mu A/cm^2$ as shown in Fig. 8b. The appearance of more corrosion sites is also evident in Fig. 8b. Visual inspection of the specimen after 288 h of exposure also showed signs of cracking in the coating.

4. Conclusions

SVET was successfully used to identify hidden delaminated areas under a coating. The state of corrosion activity

in a coated panel when exposed to Harrison's solution was monitored with exposure time. An increase in current activity with exposure was noticed for coatings which had cracked or delaminated over the exposure period. E-coat and sol–gel based coating systems showed a decrease in corrosion activity with short exposure times. The brittle 40% epoxide coating developed localized corrosion after a short exposure. The results of a short exposure of a few days may be quite misleading and this point must be kept in mind for the development of any accelerated test technique for evaluation of the corrosion resistance of advanced coatings.

Acknowledgements

References

[1] H.S. Isaacs, A.J. Aldykewicz Jr., D. Thierry, T.C. Simpson, Measurements of corrosion at defects in painted zinc and zinc alloy coated steels using current density mapping, Corrosion 52 (3) (1996) 163–168.

[2] A.J. Aldykewicz Jr., H.S. Isaacs, A.J. Davenport, The investigation of cerium as a cathodic inhibitor for aluminum–copper alloys, J. Electrochem. Soc. 142 (10) (1995) 3342–3350.

[3] H.S. Isaacs, The effect of height on the current distribution measured with a vibrating electrode probe, J. Electrochem. Soc. 138 (3) (1991) 722–727.

[4] L.B. Reynolds, R. Twite, M. Khobaib, M.S. Donley, G.P. Bierwagen, Preliminary evaluation of the anticorrosive properties of aircraft coatings by electrochemical methods, Prog. Org. Coat. 32 (1997) 31–34.

[5] L.B. Reynolds, M. Khobaib, R.S. Twite, J.C. Liang, M.S. Donley, Corrosion resistance evaluation of high performance aircraft coatings system, in: Proceedings of the 1997 Tri-Service Corrosion, Wrightsville Beach, NC, November 17–21, 1997.

[6] M. Khobaib, L.B. Reynolds, M.S. Donley, Corrosion prevention evaluation of selected sol-gel based coatings systems, Surf. and Coatings Technology, (2001) in press.